Precision Modeling and Optimally-safe Design of Quadcopters for Controlled Crash Landing in Case of Rotor Failure

Mojtaba Hedayatpour, Mehran Mehrandezh, Farrokh Janabi-Sharifi

***Abstract*— The seminal work cited in [1], [2] showed, for the first time, that flight stability of quadcopters would be possible in case of one or even multiple rotor failures. However, the quadcopter can remain airborne only by going through a spinning maneuver about an axis, fixed w.r.t the vehicle (i.e., resolved yaw). Furthermore, positional control can be achieved by periodically tilting this axis. This paper builds upon this concept with two major improvements: (1) introducing a precise aerodynamic model of propellers that takes the flapping torque due to unbalanced lifting force in the advancing and retreating blades subjected to freestream, into account, and (2) adding to the stability and flight efficiency of the quadcopter by introducing symmetric fixed tilting angles to the trust vectors. In our previous work [3], it was shown how the flight stability and energy efficiency can be improved by introducing fixed tilting angles in the thrust vectors. For controlled crash landing in case of one rotor failure, where a resolved yaw maneuver would be inevitable, introducing a titling angle in rotors can generate a reasonable resolved-rate-yaw spinning speed to keep the quadcopter airborne at a lower rotational speed of the blades by taking advantage of the freestream generated by spinning. This tilting angle would also lead to passive stability in yaw motion of the quadcopter before the failure. Our hypothesis was successfully tested via simulations.**

I. Introduction

Multicopters have gained significant attention in recent years. Due to their simplicity and maneuverability, they have been used in a broad spectrum of applications such as agronomy [4], calibrating antenna of a telescope [5] and inspection of infrastructures [6].

A special type of multicopters with four motors, known as quadcopters, has been extensively studied and there is a vast literature about their modeling, design, control and path planning. These vehicles normally have an even number of propellers half of which turn in the opposite direction of the remaining propellers. Modeling and control of a quadcopter can be found in [7].

Fault tolerant control of multicopters in case of partial or complete failure of actuators is another area of interest among researchers. For example, feedback linearization approach is used in [8] to stabilize a quadcopter after complete loss of one propeller. In [1], [2], stability and control of quadcopters experiencing one, two or three rotor failures are presented, however all propellers have parallel axes of rotation and the effects of freestream on propeller's performance were not investigated.

M. Hedayatpour is with DOT Technology Corp. Regina, Canada. M. Mehrandezh is with the Faculty of Engineering & Applied Science, University of Regina, Canada. F. Janabi-Sharifi is with the Department of Mechanical & Industrial Engineering, Ryerson University, Canada.
mojtaba@seedotrun.com, mehran.mehrandezh@uregina.ca,
fsharifi@ryerson.ca

To increase reliability via added redundancy, quadcopters with tilting rotors, hexacopters and octacopters are introduced, which are capable of maintaining stable flight despite losing one to four actuators [9], [10], however they are not optimal in terms of power consumption or stability. Research on emergency landing for a quadcopter with one rotor failure in an environment cluttered without obstacles can be found in [11], where the landing location was known a priori. However, the focus of [11] was on the design of a flight control based on a simplified dynamic model.

While most of the recent work [1], [2], [8], [11] focuse mostly on control design and stabilization, our work focuses on precision modeling, optimal design of more stable configurations of quadcopters which is of great importance in scenarios found in controlled crash landing, and high-speed flights.

In this paper, we build upon the work in [1], [2] by presenting a more realistic dynamic model of quadcopters in presence of freestream as well as investigating about a more efficient configuration, that leads to lower power consumption in hover and passive stability via resolved-rate yaw motion. We, particularly focus on a quadcopter experiencing a rotor failure and also for that in spinners. For these classes of rotary-wing UAVs, because of the fast rotation of the vehicle's body (due to unbalanced moments in the system), it is essential to consider aerodynamic effects due to freestream velocities.

First, we present a complete mathematical model of propeller's thrust force and moments and a mathematical model of quadcopter motion based on *blade element theory* [12]. Second, we utilize the hover definition presented in [2] to find the equilibrium state of the vehicle after a rotor failure by incorporating our proposed mathematical model. Third, we compare the revised equilibrium state based on our model with that of [2] in terms of power consumption in hover for different scenarios. Fourth, we propose a more efficient configuration for quadcopters (in terms of mechanical power consumption and stability) by introducing fixed tilting angles to the rotors that lead to higher passive stability in yaw motion according to our previous work in [3]. Fifth, we present the significance of our proposed aerodynamic model and mechanical configuration for quadcopters by comparing the flight data with that in the simplified quadcopter model widely used in the literature via simulations. Our results show that there exists a specific configuration for quadcopters, when adopting a fixed tilting angle in thrust vectors for each blade, that results in energy-efficient hovering via resolved-rate yaw motion in case of a single rotor failure. Last, a control strategy similar to that in [2] was utilized for

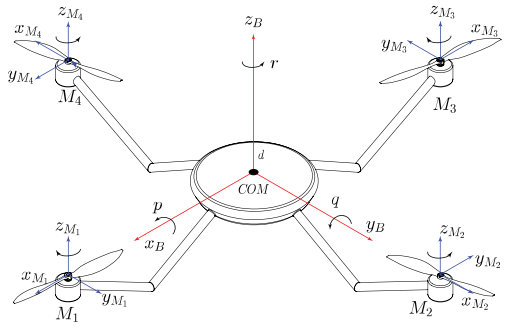

Fig. 1. Quadcopter in + configuration.

the proposed optimal configuration with fixed tilted thrust vectors and simulation results are presented.

The paper is organized as follows. In Section II, mathematical modeling of a quadcopter with a complete aerodynamic model of a propeller in presence of freestream velocity is presented. Equilibrium state after failure and effects of freestream on power consumption in hover are presented in Section III. Effects of having fixed tilted thrust vectors on power consumption and stability, a configuration with optimal-power hover solution after a rotor failure, and simulation results for controlled crash landing with the proposed optimal configuration and using the precise aerodynamic model of the propellers are presented in IV. Finally the paper concludes in Section V.

Notation: Matrices are represented by straight boldface letter and all vectors are represented by italicized boldface letters. Rotation matrix between frame i and frame j is represented by ${}^{j}\mathbf{R}_{i}$. In addition, the term ${}^{I}\omega_{B}$ denotes that ω belongs to B and is expressed in frame I. Angular velocity vector of the vehicle is represented by $\boldsymbol{\omega}^B = (p, q, r)^T$ where p, q and r are roll, pitch and yaw rates, respectively. Finally, $\|\boldsymbol{\omega}\|$ represents the 2-Norm of the vector $\boldsymbol{\omega}$ and $|s|$ represents the absolute value of scalar s.

II. Modeling

In this section a complete dynamic model of the quadcopter is given, taking the aerodynamic model of the propellers' thrust force and moments in presence of freestream into account.

Figure 1 shows the schematic of a quadcopter. Six reference frames are defined, one of which is assumed to be fixed and attached to the earth, also known as inertial frame I, one is attached to the center of mass of the vehicle and is represented by B and four other reference frames attached to the center of mass of the i^{th} motor M_i, however they do not turn with the rotors.

Each propeller generates a thrust force f_i in the direction of z-axis of the motor frame. Propellers 1 and 3 have negative and propellers 2 and 4 have positive angular velocities expressed in the body frame as $\boldsymbol{\omega}^{p_i} = (0, 0, \omega^{p_i})^T$. The moment of inertia of the propellers is approximated by that of a disk and is represented by a diagonal matrix as $\mathbf{I}^p = \text{diag}(I^p_{xx}, I^p_{yy}, I^p_{zz})$. The angular velocity of the body frame with respect to the inertial frame is represented by $\boldsymbol{\omega}^B = (p, q, r)^T$. The geometry of the vehicle is assumed to be symmetric so its moment of inertia matrix can be represented by a diagonal matrix as $\mathbf{I}^B = \text{diag}(I_{xx}, I_{yy}, I_{zz})$. The equations of motion are:

$$\mathbf{I}^B\dot{\boldsymbol{\omega}}^B + \sum_{i=1}^{4}\mathbf{I}^p\dot{\boldsymbol{\omega}}^{p_i} + \tag{1}$$

$$\text{sk}(\boldsymbol{\omega}^B)\Big(\mathbf{I}^B\boldsymbol{\omega}^B + \sum_{i=1}^{4}\mathbf{I}^p(\boldsymbol{\omega}^{p_i} + \boldsymbol{\omega}^B)\Big) =$$

$$\boldsymbol{\tau}_{\text{lift}} + \boldsymbol{\tau}_d + \boldsymbol{\tau}_{\text{reaction}} + \boldsymbol{\tau}_p,$$

$$m\ddot{\boldsymbol{d}} =^{I} \mathbf{R}_B\boldsymbol{f} + m\boldsymbol{g} + \boldsymbol{f}_d. \tag{2}$$

Where, in the left hand side of (1), the first and second terms denote the moments due to angular accelerations of body and propellers. The third term represents cross-coupling of angular momentum because of the rotation of the body and propellers and $\text{sk}(\boldsymbol{\omega}^B)$ represents the skew-symmetric matrix of the angular velocity of the body. In the right hand side of (1), the first term is the moment due to propeller's thrust force, the second term is the moment due to drag force of the fuselage, the third term is the reaction moment of the propeller and the last term is the moment due to asymmetrical lift distribution over the advancing and retreating blades of the propellers [13]. The moment due to aerodynamic drag, $\boldsymbol{\tau}_d$, is assumed to be proportional to angular velocity of the vehicle $\boldsymbol{\omega}^B$ with a proportionality constant $\mathbf{K}_d = \text{diag}(k_{dx}, k_{dy}, k_{dz})$. The reaction moment of the propeller is assumed to be proportional to the thrust force of the propeller $\boldsymbol{f}_p$, with a constant k_τ [14].

The derivation of average $\boldsymbol{\tau}_p$ and $\boldsymbol{f}_p$ are presented in our previous work [13]. They depend on blade geometry, angular velocity of the propeller, angular velocity of the vehicle and freestream velocity. Assuming a two blade propeller, we can write [13]:

$$f_p = \rho_a c C_L\Big(\frac{2R_b^3}{3}\|\boldsymbol{\omega}^p + \boldsymbol{\omega}^B\|^2 + R_b\|\boldsymbol{V}_\infty\|^2\Big), \tag{3}$$

$$\tau_p = \rho_a c C_L R_b^3\|\boldsymbol{\omega}^p + \boldsymbol{\omega}^B\|\|\boldsymbol{V}_\infty\|, \tag{4}$$

where ρ_a is the air density, c is propeller's blade chord, C_L is propeller's lift coefficient, R_b is the propeller's blade radius and $\boldsymbol{V}_\infty$ is the freestream velocity vector and is assumed to be in the $x-y$ plane of the motor frame M. From (3) and (4), it can be seen that the second term in average thrust force is proportional to the freestream velocity squared while the rolling/pitching moment of the propeller is proportional to the freestream velocity. This leads to the fact that there might be an opportunity to take advantage of freestream, especially in high speed flight (it is noteworthy that one needs to take the drag into account as well, however the drag force is normally proportional to the thrust force with a proportionality constant k_τ). Furthermore, the effects of freestream velocity must be taken into consideration in spinners and/or scenarios where a resolved-rate yaw is inevitable for flight stability (e.g., as in quadcopters with a failed rotor).

In (2), the position of the quadcopter's center of mass in the inertial frame is denoted by $\boldsymbol{d} = (d_1, d_2, d_3)$. In the right hand side, $\boldsymbol{f}$ is the sum of all the forces generated by propellers as expressed in the body frame, $\boldsymbol{f_d}$ is the aerodynamic drag force due to translational motion of the fuselage and is assumed to be proportional to the linear velocity of the center of mass of the vehicle with a proportionality constant $\mathbf{K}_D = \text{diag}(k_{Dx}, k_{Dy}, k_{Dz})$, $\boldsymbol{g}$ is the gravitational acceleration and ${}^I\mathbf{R}_B$ is the rotation matrix from body frame to inertial frame.

III. Equilibrium State For a Quadcopter Experiencing Rotor Failure

In this section, first, we derive the equilibrium state for a quadcopter experiencing a rotor failure using the method cited in [1]. However, we use our more accurate dynamic model for quadcopter and propeller for this purpose. Second, given the equilibrium state, we calculate the mechanical power for an example quadcopter and compare the results with those presented in [1]. In the end, a discussion on the results and their significance is provided.

A. Equilibrium State and Hover Solution

Generally, in multi-rotor UAVs, hovering is defined as: maintaining a position with zero angular and linear velocities. However, in case of one rotor failure in a quadcopter and in order to control the attitude and altitude of the vehicle, a new hovering definition would be required as: maintaining an altitude while rotating with constant angular velocity about a unit vector that is fixed with respect to the vehicle [1].

Suppose motor number 4 (see Fig. 1) failed. Because of the unbalanced moments of the remaining functioning propellers, the vehicle starts rotating about a unit vector $\boldsymbol{n}$ (as expressed in the body frame) with angular velocity $\boldsymbol{\omega}^B$. The evolution of this unit vector in time can be written as follows:

$$\dot{\boldsymbol{n}} = -\boldsymbol{\omega}^B \times \boldsymbol{n}. \tag{5}$$

According to this new hovering definition, we attempt to keep the orientation of this unit vector fixed with respect to the vehicle. If this unit vector is fixed, from (5) one can conclude that the angular velocity of the vehicle will remain parallel to this unit vector so the vehicle will be rotating about $\boldsymbol{n}$. If $\boldsymbol{\omega}^B$ remains constant, one can achieve hovering as long as all the states of the system will remain bounded. Also, $\dot{\boldsymbol{n}}$ must be equal to zero.

In other words, during hover, $\boldsymbol{n}$ is a unit vector stationary in the inertial frame as expressed in the body frame which is parallel to $\boldsymbol{\omega}^B$ vector. Setting (5) to zero and knowing that $\boldsymbol{n}$ is a unit vector, one can write the followings (note that an overbar indicates equilibrium values):

$$\dot{\boldsymbol{n}} = 0 \rightarrow \|\bar{\boldsymbol{n}}\| = \sigma\|\bar{\boldsymbol{\omega}}^B\| = 1 \rightarrow \sigma = \frac{1}{\|\bar{\boldsymbol{\omega}}^B\|}. \tag{6}$$

Also, during hover, the projection of total thrust forces of all propellers onto $\bar{\boldsymbol{n}}$ should balance the weight of the vehicle which results in the following:

$$\sum_{i=1}^{4} \bar{\boldsymbol{f}}_{p_i} \cdot \bar{\boldsymbol{n}} = m\|\boldsymbol{g}\|. \tag{7}$$

As the vehicle is turning with constant angular velocity $\bar{\boldsymbol{\omega}}^B = (\bar{p}, \bar{q}, \bar{r})^T$, the center of mass of the i^{th} propeller goes through a rotation about $\bar{\boldsymbol{n}}$ which generates a uniform freestream velocity $\boldsymbol{V}_\infty = \boldsymbol{l} \times \boldsymbol{\omega}^B$ over the propeller where $\boldsymbol{l}$ is the position vector of the center of mass of the propeller measured from the center of mass of the vehicle and represented in the body frame. However, since yaw is the dominant rotational motion after rotor failure, this freestream velocity can be assumed to be in the $x-y$ plane of the motor frame M and approximated by $V_\infty = \bar{r}l$ [13]. Considering this freestream velocity, using the proposed propeller model in [13] and the resultant angular velocity of the propellers, average thrust force and moment of the i^{th} propeller can be written as follows:

$$f_{p_i} = \rho_a c C_L \Big(\frac{R_b^3 {\omega^{p_i}}^2}{3} + \frac{R_b^3 \bar{r}^2}{3} + \frac{R_b \bar{r}^2 l^2}{2} + \frac{2R_b^3 \bar{r}\omega^{p_i}}{3} \Big) \tag{8}$$

$$\tau_{p_i} = \rho_a c C_L \Big(\frac{R_b^3 \bar{r} l \omega^{p_i} + R_b^3 \bar{r}^2 l}{3} \Big), \tag{9}$$

Using equations (1)- (7), by setting angular accelerations to zero and considering the proposed propeller model, a system of eight algebraic equations for 11 unknowns are obtained. Three more equations are required to solve the system. The unknowns are: $\bar{p}$, $\bar{q}$, $\bar{r}$, $\bar{n}_x$, $\bar{n}_y$, $\bar{n}_z$, σ, $\bar{\omega}^{p_1}$, $\bar{\omega}^{p_2}$, $\bar{\omega}^{p_3}$, $\bar{\omega}^{p_4}$. The first six unknowns are the components of angular velocity vector of the body and the unit vector of average thrust force of all propellers respectively, σ is the inverse of norm of the angular velocity vector $\boldsymbol{\omega}^B$ according to (6) and the last four unknowns are angular velocity of the propellers. Assuming that motor number 4 is failed ($\bar{\omega}^{p_4} = 0$) and by adding the following constraints, we will end up with a system of 11 algebraic equations with 11 unknowns. The first constraint indicates the thrust force of the propellers 1 and 3 must be equal while the second constraint means the thrust force ratio of propellers 1 and 2 must be constant.

$$\|\bar{\boldsymbol{f}}_{p_1}\| = \|\bar{\boldsymbol{f}}_{p_3}\| \ , \ \rho = \Big(\frac{\|\bar{\boldsymbol{f}}_{p_2}\|}{\|\bar{\boldsymbol{f}}_{p_1}\|} \Big)^2, \tag{10}$$

where ρ is a tuning factor and a non-negative scalar. Now there are 11 algebraic equations to be solved for 11 unknowns to find the equilibrium state. For simplicity and without compromising our precision modeling, assuming $\mathbf{I}^p \ll \mathbf{I}^B$, one can neglect the second term in (1). Also, since yaw is the dominant rotational motion, $\boldsymbol{\tau}_d$ is assumed to oppose yaw motion only and is assumed to be proportional to yaw

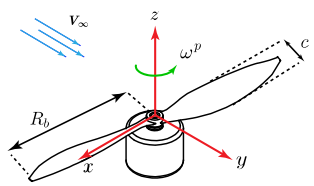

Fig. 2. Freestream velocity as represented in the $x-y$ plane of the motor frame. In this example, freestream increases relative airflow velocity over the advancing blade (on the right) and decreases it over the retreating blade which generates a pitching moment on the propeller.

rate with proportionality constant β as $\boldsymbol{\tau}_d = (0, 0, -\beta r)^T$. The reaction moment of the propeller is also assumed to be proportional to its thrust force and can be expressed in the body frame as $\boldsymbol{\tau}_{\text{reaction},p_i} = -\text{sign}(\omega^{p_i}) k_\tau \boldsymbol{f}_{p_i}$. Therefore, using the reaction moment and the angular velocity of the propeller, the mechanical power in equilibrium state can be found as follows:

$$\bar{P}_{p_i} = \bar{\tau}_{\text{reaction},p_i} \bar{\omega}^{p_i} = -\text{sign}(\omega^{p_i}) k_\tau \|\boldsymbol{f}_{p_i}\| \omega^{p_i}. \quad (11)$$

B. Hover Solutions For Example Vehicle

Next, we try to find the equilibrium state for an example vehicle with physical properties given in [1] which will be used as a base vehicle for comparing our model with that in [1] and others in which a simplified model for thrust and propeller moment was employed.

Consider a generic quadcopter (from [1]) of mass $m = 0.5$ kg, $I_{xx} = I_{yy} = 3.2 \times 10^{-3}$ kg.m^2, $I_{zz} = 5.5 \times 10^{-3}$ kg.m^2, $l = 0.17$ m, $I^p_{zz} = 1.5 \times 10^{-5}$ kg.m^2, $\beta = 2.75 \times 10^{-3}$ and $k_\tau = 1.69 \times 10^{-2}$ m. The propellers have two blades with $c = 0.03$ m, $C_L = 1.022$, $R_b = 0.08$ m and air density is assumed to be constant $\rho_a = 1.225$ kg/m^3. Note that the thrust force and reaction moment of the propellers in [1] (as well as most of the quadcopter models in the literature) are assumed to be proportional to its angular velocity squared as follows:

$$\begin{aligned} f_{p_i} &= k_f {\omega^{p_i}}^2, \\ \tau_{p_i} &= k_\tau f_{p_i}, \end{aligned} \quad (12)$$

where $k_f = 6.41 \times 10^{-6}$ Ns^2/rad^2 and k_τ are proportionality constants. In our examples, instead of k_f, we use propellers knowing $c = 0.03$ m, $C_L = 1.022$ and $R_b = 0.08$ are equivalent to k_f used in [1] to ensure fair comparison between our results with those in [1]. When freestream velocity is zero, k_f can be found as follows:

$$f_{p_i} = k_f {\omega^{p_i}}^2 = \frac{\rho_a c C_L R_b^3}{3} {\omega^{p_i}}^2 \ , \ k_f = \frac{\rho_a c C_L R_b^3}{3}.$$

For this example, without loss of generality, we assume motor number 4 is failed. Using (11) we search for an optimal-power hover solution with respect to the tuning parameter ρ. The results are presented in Fig. 3. The blue curve represents the variations of total mechanical power of the remaining functioning propellers with the simplified propeller model given in (12) while the red curve represents the same results for the improved propeller model presented in this paper.

After motor failure, we would need to calculate a value for ρ that corresponds to the minimum power hover solution using the improved propeller model. Given this value of ρ along with the solution found from (1) - (11), one can ultimately determine the angular velocity of the propellers in equilibrium state. From Fig. 3 this optimal hover solution is found when $\rho = 0$ as follows:

$$\begin{aligned} \bar{\boldsymbol{n}} = (0, 0, 1)^T, \ \bar{\omega}^{p_1} = \bar{\omega}^{p_1} = -643.7 \text{ rad/s}, \\ \bar{\omega}^{p_2} = \bar{\omega}^{p_4} = 0, \ \bar{\boldsymbol{\omega}}^B = (0, 0, 30.1)^T \text{ rad/s}, \\ \bar{f}_{p_1} = \bar{f}_{p_3} = 2.45 \text{ N}, \ \bar{f}_{p_2} = \bar{f}_{p_4} = 0, \\ \bar{P}_{\text{hover}} = \sum_{i=1}^{4} \bar{P}_{p_i} = 53.35 \text{ W}. \end{aligned} \quad (13)$$

While the minimum power hover solution for the simplified propeller model (12) is found when $\rho = 0$ as follows:

$$\begin{aligned} \bar{\boldsymbol{n}} = (0, 0, 1)^T, \ \bar{\omega}^{p_1} = \bar{\omega}^{p_1} = -618.5 \text{ rad/s}, \\ \bar{\omega}^{p_2} = \bar{\omega}^{p_4} = 0, \ \bar{\boldsymbol{\omega}}^B = (0, 0, 30.1)^T \text{ rad/s}, \\ \bar{f}_{p_1} = \bar{f}_{p_3} = 2.45 \text{ N}, \ \bar{f}_{p_2} = \bar{f}_{p_4} = 0, \\ \bar{P}_{\text{hover}} = \sum_{i=1}^{4} \bar{P}_{p_i} = 51.27 \text{ W}. \end{aligned} \quad (14)$$

Note that for different parameters and different types of propeller, as long as we are using a quadcopter, the overall shape of the graph in Fig. 3 will remain the same. Therefore, the optimal power hover solution occurs at $\rho = 0$ as found in (13) and (14). Also, it is worth mentioning that for $\rho > 1$ the total mechanical power is far from being optimal and are not included in the figure for brevity.

C. Discussion

After a rotor failure, the vehicle starts spinning with angular velocity $\boldsymbol{\omega}^B$ which will be in the opposite direction of rotation of some of the propellers. Therefore, these propellers need to turn faster to generate the same thrust force as that before the failure which leads to higher mechanical power. This is particularly important, when the angular velocity of the body is not negligible compared to that of the propellers.

Figure 3 presents another interesting result. While searching for the optimal power hover solution with respect to ρ, we find that the total mechanical power for hover solution when $\rho = 0.45$ is very close to that when $\rho = 0$ when using the improved propeller model. However, there is a subtle difference between these two cases, which we beleive it reflects on the controllability of the vehicle.

Another conclusion can be drawn using (8) and (9) as: higher freestream velocities may result in lower mechanical power consumed during hover, which is due to the thrust force being proportional to the freestream velocity squared. In addition, in case of a rotor failure with yaw being the dominant rotational motion, this freestream velocity, being proportional to the angular velocity of the vehicle $\bar{r}$. As stated

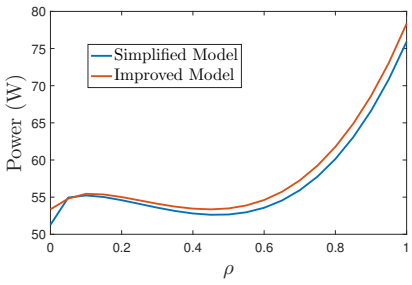

Fig. 3. Variations of mechanical power versus variations of ρ for a quadcopter experiencing a rotor failure. Note that $\rho = 0$ represents the case where rotors 1 and 4 are failed as well.

earlier, $\bar{r}$ has an adverse effect on total mechanical power only if it is in the opposite direction of the propeller's angular velocity ω^p. As a result, if we find a configuration where $\bar{r}$ and ω^p are in the same direction (either after a rotor failure or in a spinning UAVs) then we can get the best of both worlds. In the next section, we present some results on how to find this configuration.

IV. Effects of Tilting The Rotors

This section presents the effects of tilting the rotors of the quadcopter on mechanical power as well as finding optimal-power configurations for quadcopters experiencing a rotor failure. Note that this tilting angle will be fixed for each configuration and does not change on the fly, therefore no additional actuator is required.

In regular quadcopters, yaw motion is usually carried out by reaction moments of the rotors. This moment is fairly small compared to the that generated by the propeller's thrust force about the center of mass of the vehicle, therefore it may not be an efficient way to induce yaw. Instead, one can yaw by tilting the rotors by an angle α about the x-axis of their corresponding motor frame, thus, using a small component of the propeller's thrust force to generate relatively larger yaw moments. Note that the tilting angle should be small enough ($-0.2 < \alpha < 0.2$ rad) so that (8) and (9) still hold true and the component of the thrust force that balances the weight of the vehicle experiences relatively small changes.

We introduce a tilting angle α_i about the x-axis of the motor frame M_i to the rotors similar to that in [3] as shown in Fig. 4. According to [3], having $\alpha_{1,3} > 0$ and $\alpha_{2,4} < 0$ adds to the passive stability of the vehicle in yaw motion which is an improvement in quadcopter flight without any rotor failure. But we are interested in finding the effects of this tilting angle on the mechanical power of the quadcopter after rotor failure and also on spinning UAVs like bispinner.

A new configuration is proposed by tilting the rotors about the x-axis of the motor frame (shown in blue in Fig. 1) as shown in Fig. 4 (a) where the positive direction of the tilting angle α_i is shown in Fig. 4 (b). Because rotors 1 and 3 are assumed to be turning in the negative direction of z-axis of the body frame, by tilting these motors by any positive angle, the vehicle tends to generate a yaw motion that is in favor of reducing mechanical power (11). Whereas for rotors 2 and 4 which are turning in the positive direction of the z-axis of the body frame, the tilting angle should be negative. Note that, for simplicity, it is assumed $|\alpha_1| = |\alpha_2| = |\alpha_3| = |\alpha_4|$.

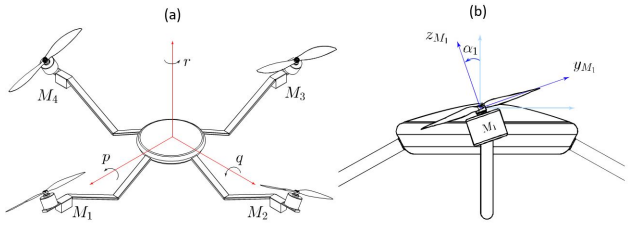

Fig. 4. (a) a new configuration with tilted rotors. (b) the positive direction of the tilting angle α.

Although this new configuration might not lead to reducing mechanical power in quadcopters without rotor failure very effectively, however, it can be drastically useful in quadcopters experiencing rotor failure and in spinning UAVs. Another question that might be asked is about the application of spinning UAVs. An interesting application of spinning UAVs is invisible flight for surveillance purposes. One example is *Phantom Sentinel*, a hand launch spinning UAV, developed and patented by *VeraTech Aero Corporation* [15].

For the quadcopter example, Assuming motor number 4 is failed, we search for the best set of ρ and α using (11) to find the optimal-power hover solution. Results show that the minimum-power solution can be found when $\rho = 0$ and $\alpha_{1,3} = -0.2$ rad. When $\rho = 0$, motor number 2 is also off and it means we only have a bispinner configuration. If we solve equations (1)- (10) for $\rho = 0$ and $\alpha_{1,3} = -0.2$, the hover solution can be found as follows:

$$\begin{aligned} \bar{\boldsymbol{n}} = (0,0,1)^T,\ \bar{\omega}^{p_1} = \bar{\omega}^{p_1} = -588.9 \text{ rad/s}, \\ \bar{\omega}^{p_2} = \bar{\omega}^{p_4} = 0,\ \bar{\boldsymbol{\omega}}^B = (0,0,-30.7)^T \text{ rad/s}, \\ \bar{f}_{p_1} = \bar{f}_{p_3} = 2.50 \text{ N},\ \bar{f}_{p_2} = \bar{f}_{p_4} = 0, \\ \bar{P}_{\text{hover}} = \sum_{i=1}^{4} \bar{P}_{p_i} = 49.80 \text{ W}. \end{aligned} \tag{15}$$

By comparing (15) with (13), it can be seen that although propellers 1 and 3 in (15) are turning slower, they are generating more thrust force than those in (13). This is because the body of the quadcopter in (13) is turning in the opposite direction of propellers 1 and 3, therefore the propellers have to turn faster to generate the same amount of thrust force. In other words, the resultant angular velocity of the propeller with respect to the freestream is important, not the absolute rotational speed of the rotors.

A. Discussion

All the hover solutions for case studies presented in this paper come with relatively high angular velocity $\bar{\boldsymbol{\omega}}^B$. This means that after a rotor failure in quadcopters, for stabilization, the controller must be able to bring the vehicle from rest before the failure (assuming it is in hover) to the new equilibrium state where the vehicle spins with constant angular velocity $\bar{\boldsymbol{\omega}}^B$. Specifically, this is non-trivial when using linear control strategies for stabilization at high angular velocities and bringing the vehicle from stationary state to the new equilibrium state [1], [2].

In addition, to control the attitude and position of the vehicle, we should manipulate the angular velocity of the propellers periodically and at a frequency higher than or equal to the corresponding frequency of the periodic motion of the vehicle. Therefore, the motors turning the propellers must be capable of responding at such high frequencies. This itself adds another constraint to the problem.

Another issue may arise in hover solutions where the angular velocity of the body is slower than a certain threshold which could result in the vehicle rendering itself uncontrollable (see controllability conditions given in [2]).

The introduced tilting angle to the thrust vectors resolves the aforementioned issues with the hover solutions presented

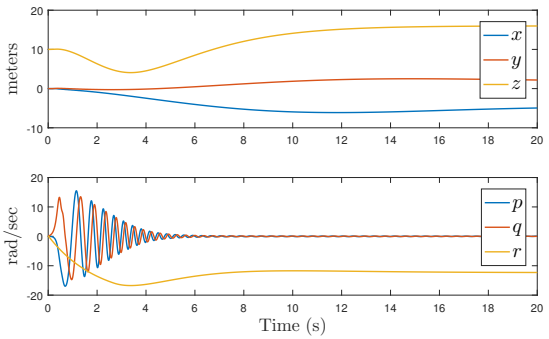

Fig. 5. Simulation results for position control. $\boldsymbol{d}_0 = (0, 0, 10)$ m and $\boldsymbol{d}_{des} = (-5, 2, 16)$ m.

earlier. It allows us to explore more configurations and find a hover solution where the frequency of the periodic motion in hover is less than the frequency at which we command the motors. It also helps us to find a configuration that is both controllable after rotor failure and its hover solution is close enough to the equilibrium state of the vehicle before the failure such that linear control strategies can be applied for stabilization.

By choosing this tilting angle to be $\alpha_{1,3} = -0.14$ rad, the following hover solution can be found:

$$\begin{aligned} \bar{\boldsymbol{n}} = (0, 0, 1)^T,\ \ \bar{\omega}^{p_1} = \bar{\omega}^{p_1} = -608.5 \text{ rad/s}, \qquad (16) \\ \bar{\omega}^{p_2} = \bar{\omega}^{p_4} = 0,\ \bar{\boldsymbol{\omega}}^B = (0, 0, -12.3)^T \text{ rad/s}, \\ \bar{f}_{p_1} = \bar{f}_{p_3} = 2.48 \text{ N},\ \bar{f}_{p_2} = \bar{f}_{p_4} = 0, \\ \bar{P}_{\text{hover}} = \sum_{i=1}^{4} \bar{P}_{p_i} = 50.93 \text{ W}. \end{aligned}$$

Although (16) is not as energy-efficient as (15), it leads to having an angular velocity $\boldsymbol{\omega}^B$ that is lower than that in (14) and allows us to use linear control strategies.

Finally, to demonstrate feasibility of the hover solution and validate the results, we present simulation results for position and attitude control for the quadcopter in (16) after a rotor failure in Fig. 5. Using the control strategy from [1], an LQR controller, with a weight matrix $\mathbf{Q} = \text{diag}(1, 1, 20, 20)$ on the attitude states p, q, n_x and n_y and a weight of $R = 1$ for the control input, is designed. The first graph represents the position of the quadcopter starting from an initial position $\boldsymbol{d}_0 = (0, 0, 10)$ m to a desired position $\boldsymbol{d}_{des} = (-5, 2, 16)$ m. The second graphs represents the components of angular velocity vector of the body as expressed in the body frame. The higher frequency response in pitch and roll motion is because only these two rotational degrees of freedom are manipulated directly to control the x and y components of the position of the vehicle. Please note that we used a linear control strategy and could successfully stabilize the vehicle.

V. Conclusions

This paper presents precision modeling and optimal-power hover solutions for quadcopters experiencing rotor failures and for spinning UAVs. A complete dynamic model is presented considering the effects of freestream on propeller's thrust force and moments. Hover solutions for a quadcopter experiencing a rotor failure is presented next and its mechanical power is computed and compared with that for a quadcopter with simplified propeller model widely used in the literature. The results show that the simplified propeller model cannot approximate the thrust force and moments of the propeller accurately enough. The differences between the two models are presented. We introduced a fixed tilting angle to the rotors which helps to find more power optimal hover solutions for quadcopters experiencing rotor failure. Results show that this fixed tilting angle also helps in controllability of the vehicle and finding more feasible configurations for spinning UAVs. In the end, example simulation results are presented.

References

[1] M. W. Mueller and R. D'Andrea, "Stability and control of a quadrocopter despite the complete loss of one, two, or three propellers," in *IEEE International Conference on Robotics and Automation (ICRA)*, Hong Kong, 2014, pp. 45–52.

[2] ——, "Relaxed hover solutions for multicopters: application to algorithmic redundancy and novel vehicles," *International Journal of Robotics Research*, vol. 35, no. 8, pp. 873–889, 2015.

[3] M. Hedayatpour, M. Mehrandezh, and F. Janabi-Sharifi, "A unified approach to configuration-based dynamic analysis of quadcopters for optimal stability," in *2017 IEEE/RSJ International Conference on Intelligent Robots and Systems (IROS)*, Vancouver, Canada, 2017, pp. 5116–5121.

[4] J. Rasmussen, J. Nielsen, F. Garcia-Ruiz, S. Christensen, and J. C. Streibig, "Potential uses of small unmanned aircraft systems (uas) in weed research," *Weed Research*, vol. 53, no. 4, pp. 242–248, 2013.

[5] J. R. Horandel, S. Buitink, A. Corstanje, J. E. Enriquez, and H. Falcke, "The lofar radio telescope as a cosmic ray detector," in *International Cosmic Ray Conference*, 2013.

[6] J. Thomas, J. Polin, K. Sreenath, and V. Kumar, "Avian-inspired grasping for quadcopter micro uavs," *Bioinspiration & Biomimetics*, vol. 9, pp. 25 010–25 019, 2014.

[7] S. Bouabdallah and R. Siegwart, "Full control of a quadcopter," in *IEEE/RSJ International Conference on Intelligent Robots and Systems*, San Diego, CA, 2007, pp. 153–158.

[8] A. Freddi, A. Lanzon, and S. Longhi, "A feedback linearization approach to fault tolerance in quadrotor vehicles," in *Proceedings of the 18th IFAC world congress*, 2011, pp. 5413–5418.

[9] M. Ryll, H. H. Bulthoff, and P. R. Giordano, "Modeling and control of a quadcopter uav with tilting propellers," in *IEEE International Conference on Robotics and Automation (ICRA)*, Saint Paul, MN, 2012, pp. 4606–4613.

[10] A. Marks, J. F. Whidborne, and I. Yamamoto, "Control allocation for fault tolerant control of a vtol octorotor," in *Proceedings of 2012 UKACC International Conference on Control*, 2012, pp. 357–362.

[11] V. Lippiello, F. Ruggiero, and D. Serra, "Emergency landing for a quadrotor in case of a propeller failure: A backstepping approach," in *IEEE/RSJ International Conference on Intelligent Robots and Systems*, Chicago, IL, 2014, pp. 4782–4788.

[12] J. D. Anderson, *Fundamentals of Aerodynamics*, 5th ed. United States: McGraw Hill Higher Education, 2016.

[13] M. Hedayatpour, M. Mehrandezh, and F. Janabi-Sharifi, "Propeller performance in presence of freestream: Applications in modeling multirotor uavs," in *Advances in Motion Sensing and Control for Robotic Applications*, F. Janabi-Sharifi and W. Melek, Eds. Cham: Springer International Publishing, 2019, pp. 45–60.

[14] P. Martin and E. Salaun, "The true role of accelerometer feedback in quadrotor control," in *2010 IEEE International Conference on Robotics and Automation*, Anchorage, AK, 2010, pp. 1623–1629.

[15] VeraTech Corporation. [Online]. Available: http://veratech.aero/phantom.html